Structural features of $(Ba_2Cu_2O_{4+x})/(CaCuO_2)_n$ superconducting oxide superlattices with ultrathin individual layers

G. Balestrino, G. Pasquini,* and A. Tebano
INFM–Università di Roma ''Tor Vergata,'' Dipartimento di Scienze e Tecnologie Fisiche ed Energetiche, Via di Tor Vergata 110, 00133 Roma, Italy
(Received 3 February 2000)

The structural disorder in $(Ba_2Cu_2O_{4+x})/(CaCuO_2)_n$ superlattices with ultrathin individual layers consisting of a noninteger number of unit cells is investigated. X-ray diffration and reflection high energy electron diffraction show that a two-dimensional layer by layer growth occurs and that layers of mixed composition are corrugated to adjust the internal stresses. On the basis of these conclusions we can outline an explanation for the behavior of T_c vs n in $(Ba_2Cu_2O_{4+x})/(CaCuO_2)_n$ superlattices.

I. INTRODUCTION

Presently, considerable attention is being addressed to the engineering of artificial structures based on ultrathin individual layers consisting of complex oxides. In this framework ferroelectric,[1] colossal magnetoresistance,[2,3] high temperature superconducting[4,5] oxide superlattices have been extensively studied due to their scientific importance and technological interest. Fabrication of such artificial structures, with a control on the atomic layer level, can allow to improve the physical properties of such oxides and, in perspective, can be used to design devices with new functional properties.[6] Obviously, in order to achieve such objectives, an extremely careful control of the interface disorder during the growth procedure is necessary. Interface disorder control is usually achieved by *in situ* reflection high energy electron diffraction[7] (RHEED) or by *ex situ* techniques such as x-ray diffraction[2,5,8] (XRD) or high resolution transmission electron microscopy (HRTEM).[2] RHEED technique, through the detection of the intensity oscillations of the diffraction spots, is a powerful tool for the control of the layer thickness and interface quality. However, even for a purely two-dimensional (2D) growth mode, clear RHEED oscillations cannot always be detected. Moreover, the oxygen pressure necessary for the growth of oxide layers could hinder the use of the RHEED technique. In such cases *ex situ* techniques are necessary. For this respect, HRTEM is a powerful technique to enlighten the local structure of the interfaces. On the other hand, XRD gives information averaged over the whole superlattice thickness. At the simplest level XRD spectra can be used to estimate the superlattice period Λ and the individual thickness of the constituent layers. In the case of two constituent oxides, the superlattice period Λ ($\Lambda = n_1 c_1 + n_2 c_2$ where c_1 and c_2 represent the thickness of the unit deposition cell of the two constituent oxides and n_1 and n_2 the respective number of unit cells) is calculated from the angular spacing between the zeroth order peaks (SL_0) of the superlattice and the first order satellite peaks ($SL_{\pm 1}$) using the equation $\Lambda = \lambda/(2|\sin\theta_{\pm 1} - \sin\theta_0|)$, where λ is the x-ray wavelength, θ_0 and $\theta_{\pm 1}$ are the angular position, respectively, of the average structure peak and of the first order satellite peaks. The average lattice parameter $\overline{c} = \Lambda/(n_1 + n_2)$ can be estimated from the angular position of the average structure peaks by Bragg's law. Finally, assuming the c_1 and c_2 values are known independently, the individual layer thicknesses n_1 and n_2 can be calculated. This approach has been extensively applied to the study of metallic,[9] semiconducting,[8] and, more recently, oxide superlattices.[2,4] Often, following this simple procedure, noninteger values of n_1 and n_2 were found.[2,4,8] In the case of the manganites superlattices, investigated in Ref. 2, HRTEM images have clearly shown that the structural quality of the topmost layer is not deteriorated, relative to the first layer, even in the case of noninteger individual layer thicknesses. In the past, individual layers made of noninteger numbers of unit cells were first observed in the case of semiconducting superlattices.[10] This effect was successively explained on the basis of interfacial *controlled disorder*[8] due to a systematic error in the thickness of the deposited layers. However, especially in connection with complex oxide superlattices, where the unit deposition cell (thinnest block of a single constituent oxide which can be deposited) may consist of several atomic planes and may differ strongly from each other both in chemical composition and crystallographic structure, the ideas of interfacial disorder[9,11] have to be reconsidered. This is especially true in the case of artificial structures made of ultrathin layers consisting of few (or even one) unit deposition cells where the concept of interface itself becomes ill defined.

In this paper we discuss the case of the $(Ba_2Cu_2O_{4+x})/(CaCuO_2)_n$ superlattices grown by pulsed laser deposition (PLD).[4] These superlattices, grown under appropriate temperature and oxygen pressure conditions, can have a superconducting transition temperature T_c as high as 80 K.[12] All their superconducting properties are drastically affected by the large degree of structural disorder present.[13]

Recently it has been shown by EXAFS and x-ray diffraction measurements in $(Ba_2Cu_2O_{4+x})/(CaCuO_2)_n$ superlattices[14,15] that the crystallographic structure of the Ba block consists of a sequence of four atomic planes, namely $CuO_2/BaO/Cu_{1-\delta}O_x/BaO$ with $c_1 = 8.9$ Å. The Ca block consists of a sequence of CuO_2 and Ca planes and has a true *infinite layer* (IL) structure with $c_2 = 3.2$ Å.[16] The Ba block contains x extra oxygen ions and, therefore, can act as a *charge reservoir* (CR) block. The coexistence, in a single structure, of CR and IL blocks regularly stacked along the growth direction gives rise to superconductivity. The behavior of the superconducting transition temperature T_c of

$(Ba_2Cu_2O_{4+x})_1/(CaCuO_2)_n$ superlattices as a function of n (calculated according the procedure outlined above), has been reported in Ref. 12. The maximum T_c value is obtained for $2 \lesssim n_{opt} \lesssim 2.5$. For larger n values, $T_c(n)$ shows a smooth decrease, which is well explained taking into account the decrease of the effective hole concentration per single CuO_2 plane due to the increase of the total number of CuO_2 planes in the IL block.[17] For $n<2$, T_c shows a sharp drop. A striking result of this investigation was that the occurrence of a non integer number n of $CaCuO_2$ unit cells in the IL block does not affect the T_c of these artificial structures.

The aim of this work is to characterize, by means of a simple kinematic analysis of the x-ray diffraction spectra, the structural disorder of these artificial materials with the final objective of correlating the superconducting properties with the structural disorder.

To achieve this goal, different kinds of disorder are considered. X-ray diffraction spectra are accordingly simulated for n ranging from 2 to 3 (where the maximum of T_c is observed) and finally compared with the experimental results. Conclusions are compared with the results of RHEED *in situ* experiments. A possible explanation for the dependence of T_c on n is sketched.

II. EXPERIMENTAL RESULTS

$[(Ba_2Cu_2O_{4+x})/(CaCuO_2)_n]_N$ superconducting superlattices were grown onto $SrTiO_3$ (100) monocrystalline substrate by the PLD technique following the procedure described in Ref. 4. N is the total number of iterations in the deposition process (typically 30 in our superconducting superlattices, corresponding to a total thickness of about 450 Å). Samples were characterized by x-ray diffraction and standard four contact transport measurements. Samples with the same composition were also grown at low molecular oxygen pressure ($P_{O_2} \sim 10^{-4}$ mbar) in order to investigate the growth mechanism by *in situ* RHEED.

X-ray diffraction spectra were taken by a θ-2θ diffractometer.

Figure 1 shows in logarithmic scale the experimental x-ray diffraction spectra (open circles) corresponding to four different samples with n ranging between 2 and 3. n was varied increasing gradually the number of laser shots on the $CaCuO_2$ target. From the figure it can be noticed that, increasing n, the spectrum is modified as follows.

The zeroth order peaks SL_0, (001) and (002) are displaced to larger angles.

The angular distance between the zeroth order and first order satellite peaks decreases as Λ increases.

The $SL_{\pm 2}$ satellite peak of the $n=2$ sample splits gradually in a SL_{+2} and a SL_{-2} peak.

No relevant broadening of the $SL_{\pm 1}$ and SL_0 peaks is observed for superlattices with noninteger values of n.

The $SL_{\pm 2}$ peaks, on the contrary, are much weaker and broader when n has noninteger values.

In the case of superlattices grown at low oxygen pressure, the growth was monitored by the RHEED technique. RHEED spectra showed that the growth occurs in a 2D mode without degradation of the superlattice quality over the whole thickness. In Fig. 2 a typical 2D pattern taken at the end of the growth is shown.

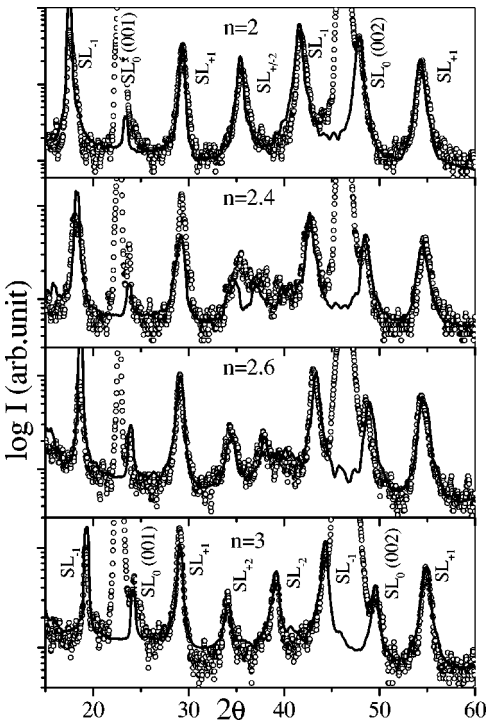

FIG. 1. Experimental x-ray-diffraction spectra shown in logarithmic scale (open circles) corresponding to four different samples with n ranging between 2 and 3 and the corresponding simulated spectra (continuous line) obtained by the final structural model. The $S_{\pm 2}$ peak splits gradually. Experimental strong peaks come from the $SrTiO_3$ substrate.

III. SIMULATION MODELS

Numerical simulations of the XRD experimental spectra were carried out following a kinematical approach. Such approximation is well justified in view of both the reduced thickness of the superlattices and of their crystallographic

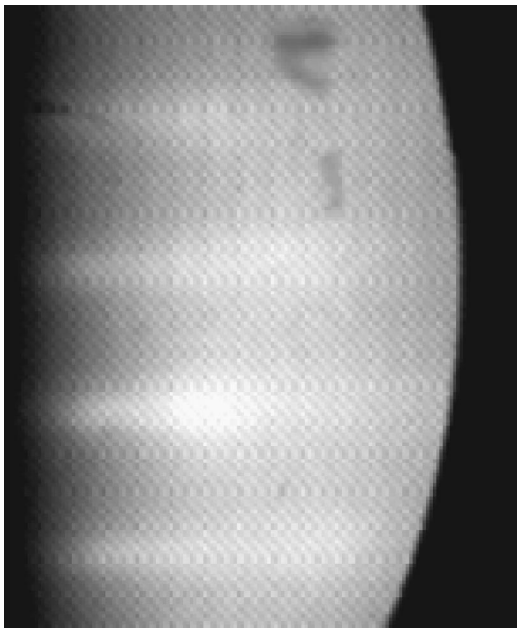

FIG. 2. RHEED image taken at the end of the growth. A 2D streaky pattern is still clearly visible.

quality. In this simple approximation the diffracted intensity at the angle θ, $I(\theta)=A(\theta)A^*(\theta)$, is calculated by the expression

$$A(\theta)=\sum_j f_j(\theta)\exp(-i4\pi z_j \sin(\theta)/\lambda), \qquad (1)$$

where j indexes the atomic planes and $f_j(\theta)$ is the structure factor (including anomalous dispersion correction) corresponding to atoms lying in the jth plane. The z_j is the height of the jth plane and λ represents the wavelength of the Cu $K\alpha$ radiation. The sum is carried out over the whole thickness of the film. The structure factor has been corrected by the polarization and Lorentz factors and by the Debye-Waller temperature factor. The f_j and z_j values depend on the particular structural model utilized.

For a comparison with the experimental curves the final spectrum is convoluted with the 0.5° window used in the x-ray measurements and the background intensity is added.

In Ref. 8 the concept of *controlled disorder* in a 2D layer by layer growth was introduced in the case of GaAs/AlAs semiconducting superlattices. *Controlled disorder* occurs when the amount of material deposited in each iteration remains perfectly constant during the growth of the superlattice even though it does not correspond to an integer number of atomic planes. In a pure layer by layer 2D growth model any layer must be completed before passing to the next one (Frank–Van der Merve growth). Consequently, the composition of the interface is always well defined, and varies in a controlled fashion throughout the film thickness.

On the other hand, *random disorder* can be produced by a poor control of the amount of deposited material in each iteration or by a nonideal 2D growth without surface reconstruction over large areas.

In the case of superlattices made of complex oxides, the above ideas about the growth mechanisms can be applied as well. However, some special features, due to the more complex structure of these compounds, must be considered.

(a) The constituent oxides can grow block by block rather than atomic plane by atomic plane, each unit block consisting of several atomic planes.

(b) Large structural differences between the constituent oxides may exist.

Both these features occur in the case of the $[(Ba_2Cu_2O_{4+x})/(CaCuO_2)_n]_N$ superlattices.

We have simulated the x-ray spectra for different possible disorder models for $n=2$, 2.4, 2.6, and 3. In Fig. 3 the XRD experimental spectrum of a $[(Ba_2Cu_2O_{4+x})/(CaCuO_2)_{2.4}]_N$ superlattice is compared with the simulation obtained in the most relevant cases. All spectra are plotted in logarithmic scale.

Figure 3(a) shows the result of a simple random disorder model. In this simulation, it has been supposed that, in each growth domain, the $CaCuO_2$ layer can consist only of an integer number of unit cells, with a probability $P=0.6$ to have 2 cells, and $P=0.4$ to have 3 cells. No correlation exists between successive $CaCuO_2$ layers in each domain (nonideal 2D growth). Furthermore, in order to take into account the experimental fluctuations in the amount of deposited material, a further random disorder has been incorporated considering a Gaussian dispersion in the above probabilities.

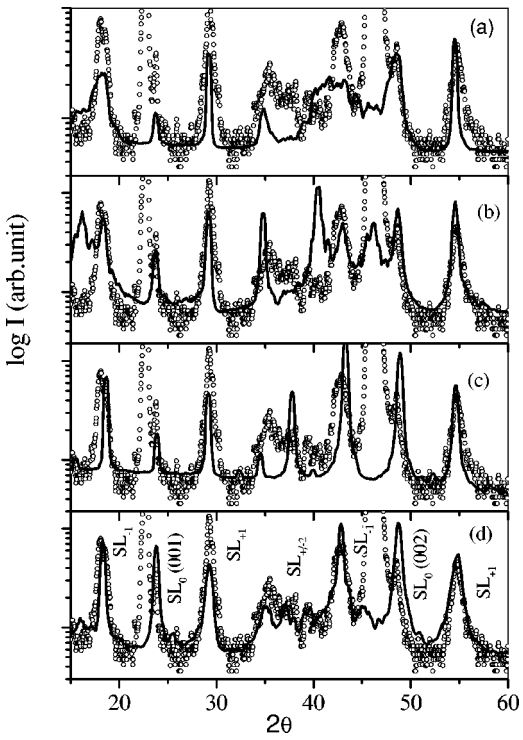

FIG. 3. XRD experimental spectrum in logarithmic scale of a superlattice with $n=2.4$ (open circles) compared with the simulated spectra (continuous line) obtained from different structural models. (a) Simple random disorder model with nonideal 2D growth. (b) 2D growth model with abrupt steps in the deposition planes [Fig. 4(a)]. (c) 2D growth model with constant thickness unit deposition layers [Fig. 4(b)]. (d) Final model.

This model, similar to the one considered previously for (Ba-Cu-O)/(Sr-Cu-O) superlattices,[18] works quite well for samples with integer n but fails in the other cases. It can be seen in Fig. 3(a) that experimental and simulated spectra are qualitatively different. In the simulation, the SL_{+1} peaks are very narrow while the SL_{-1} peaks are broad. No split is observed for the $SL_{\pm 2}$ peak.

Such disagreement is expected on the basis of the RHEED characterization, which shows that the growth mechanism has a 2D character. Therefore a 2D growth model which allows the preservation of the real structure of the Ba block ($Ba_2Cu_2O_{4+x}$) has to be considered. In this specific case, the unit deposition layers (UDL) must be completed sequentially one by one. UDL (the thinnest layer which can be grown from a single target) consist, in our case, of an alkaline earth plane and a copper plane.

In such a model, two extreme possibilities, illustrated in Fig. 4, can be envisaged for the UDL with mixed composition.

(1) The unit cell of each constituent oxide maintains its relaxed dimensions. Due to the large difference between the Ba-Ba (4.4 Å), Ba-Ca (3.8 Å), and Ca-Ca (3.2 Å) distances, this situation implies the existence of abrupt steps in the atomic planes [black lines in Fig. 4(a)] at the boundaries between regions of different composition.

(2) The thickness of each mixed composition UDL is constant and can be calculated by the Vegard' law from the average chemical composition. This approximation has been used successfully for semiconducting superlattices with non-

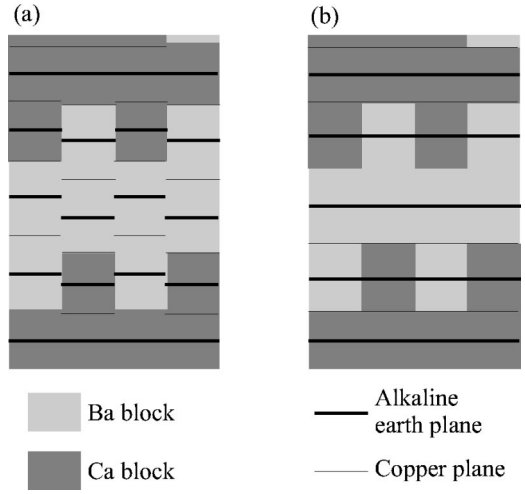

FIG. 4. Sketch of a small portion of a superlattice built according to the 2D growth extreme models. (a) The unit cells maintain their relaxed dimensions and abrupt steps in the deposition planes result. (b) The thickness of each unit deposition layer is constant and can be calculated by the Vegard' law.

integer composition.[8] In the present case, however, we have also included the restriction of maintaining the structure of the $(Ba_2Cu_2O_{4+x})$ block [Fig. 4(b)].

Simulated spectra for $n=2.4$ resulting from the above extreme cases are shown in Figs. 3(b) and 3(c). Clearly the first alternative [Fig. 3(b)] gives rise a spectrum very different from the experimental one.

The second possibility [Fig. 3(c)] gives rise a simulated spectrum qualitatively better. The SL_{-1} peaks are in the correct position and the $SL_{\pm 2}$ peak is split. The relative intensities and widths of $SL_{\pm 1}$ and SL_0 peaks are better reproduced. However, in the simulated spectrum the $SL_{\pm 2}$ peaks are as narrow as the other ones in disagreement with the experimental observation. This is indicative of an underestimate of the interfacial disorder of the superlattice.

We have tried then to model a more realistic intermediate alternative. This model is based on the physical assumption that Ca and Ba blocks are distorted in order to avoid sharp steps and to create smooth and continuous surfaces. Each jth plane has a variable local height which depends on the overall history of the growth.

More specifically the key physical features that we consider in the final model are as follows.

(1) The growth mechanism is 2D: UDL must be completed sequentially one by one. In the case of mixed composition UDL, 2D islands made of the first constituent oxide start to enucleate on the surface without reaching the full coverage, UDL is then completed with the second constituent oxide.

(2) In mixed composition UDL, cells are locally distorted at the boundaries between different composition regions, in order to form smooth and continuous growth surfaces.

(3) Far from the boundaries between regions of different composition the UDL thickness tends to recover its relaxed value.

(4) The structural identity of the Ba block, as determined from the EXAFS measurements, is preserved.

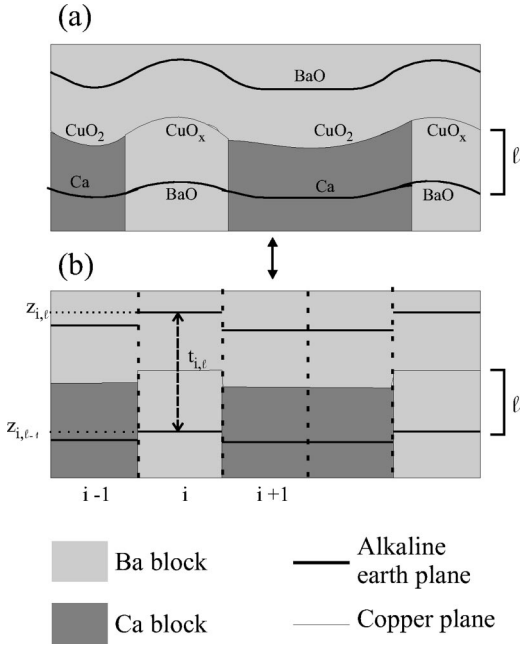

FIG. 5. (a) Sketch of a portion of a superlattice built according to the 2D growth final model. Layers are corrugated to adjust the internal stresses. (b) Simplified discrete 1D model structure corresponding to the situation depicted in (a).

(5) Random fluctuations in the amount of material deposited in each iteration give rise to an additional random disorder component.

A small region of a superlattice grown according the mechanism outlined above is sketched in Fig. 5(a). In order to perform numerical simulation of the x-ray diffraction spectra, a simplified 1D model structure has been considered [Fig. 5(b)]. This simplified model considers several growth domains (numerated by the letter i).

Each UDL (numerated by the letter l) consists of an alkaline earth plane (indicated by black thick lines in the figure) and a copper plane (thin lines). In each UDL, domains are completely filled either with a Ca block (dark gray regions) or with a Ba block (light gray regions). In each deposition, n_{Ba} and n_{Ca} take random values that follow a Gaussian distribution with dispersion σ around the mean values $\langle n_{\mathrm{Ba}}\rangle = 1$ and $\langle n_{\mathrm{Ca}}\rangle = n = 2,2.4,\ldots$. In this simplified model, each UDL domain has a constant thickness [Fig. 5(b)] which can be thought to represent the mean thickness value of the corresponding portion of the real undulated growth surface [Fig. 5(a)].

If the crystallographic cells are completely distorted and the surfaces are very smooth, the resulting steps would be very small. On the other hand, if the cells are very stiff, the situation should be similar to the first extreme case [Fig. 4(a)] and the steps would be higher. In the numerical procedure, the ''surface smoothness'' is adjusted by means of a smoothing parameter s defined thereafter. The thickness t_{il} of each (i,l) domain, starting for the first UDL, is redefined as

$$t_{il} = t^o_{il} + s/4[2(z_{i,l-1} + t^o_{i,l}) - (z_{i+1,l-1} + t^o_{i+1,l}) - (z_{i-1,l-1} + t^o_{i-1,l})]$$

where $t^0_{i,l}$ is the ideal relaxed thickness. The parameter s can vary from 0 to 1. $s=0$ corresponds to the extreme case de-

picted in Fig. 4(a). Finally we take into account interference among different UDL domains performing the sum expressed in Eq. (1) over all domains

$$A(\theta)=\sum_{ji} f_{ji}(\theta)\exp(-i4\pi z_{ji}\sin(\theta)/\lambda). \qquad (2)$$

A very good agreement between the calculated and experimental spectra has been obtained for values of σ around the 10% of n and $s=0.5$. The resulting simulated spectra are shown in Fig. 3(d) for $n=2.4$ and in Fig. 2 for $n=2$, 2.4, 2.6, and 3.

IV. DISCUSSION AND FINAL CONCLUSIONS

X-ray spectra simulations demonstrate that, for these artificial structures, a 2D layer by layer growth is achieved. In the case of mixed composition layers the 2D growth starts with the first constituent oxide and is completed, still in a 2D mode, by the second constituent. Therefore the mixed unit deposition layers (UDL) consist of small regions of different compositions. This result is in agreement with the finding of the *in situ* RHEED measurements which show no sizeable deterioration of the surface during the deposition. Moreover, HRTEM experiments with atomic resolution in oxide superlattices of different nature, show that, actually, the quality of layers close to the physical surface of the film is comparable with that one of the first layer.[2]

The second conclusion is that, in each mixed composition UDL, cells are distorted to avoid sharp height steps, however such distortion is not enough to establish a constant thickness throughout the UDL. This is also in agreement with the HRTEM experiments published in Ref. 2, which show an undulation of the interfaces.

Simulated spectra fit the x-ray experiments better if the structure of the ($Ba_2Cu_2O_{4+x}$) block is maintained. This finding gives further support to the EXAFS results.

We notice also that, to reproduce accurately the peak widths, it is necessary to take into account an experimental dispersion in the amount of material deposited in each iteration.

Finally we analyze the implications that this structural model could have on the superconducting behavior of these materials.

The sharp drop of $T_c(n)$ when $n<2$ can be explained assuming that, in this compounds, the thinner superconducting block consists of a CuO_2 plane surrounded by two alkaline earth planes. If the last is true, the explanation for the good superconducting properties of fractional superlattices emerges naturally. Namely, superconducting blocks in samples with n slightly larger than 2 are more ordered relative to those with $n=2$. The presence of random disorder prevents the existence of ordered superconducting blocks in the $n=2$ samples. As far as n increases, there are more superconducting blocks. The competition between this effect and the decrease of the number of holes per CuO_2 plane, could explain the maximum of T_c observed for $2<n<2.5$. However, such hypothesis still needs a more detailed investigation in samples with different degrees of random disorder.

In summary, from the comparison between different disorder models we have inferred the key structural features necessary to reproduce the x-ray spectra observed in these superconducting artificial materials. We have proposed a simple model that captures these physical facts.

The conclusions emerging with respect to the structure and growth mechanism of these artificial materials are in agreement with the observations of RHEED and HRTEM experiments in similar compounds.

On the basis of these conclusions we can outline an explanation for the $T_c(n)$ behavior. This explanation is valid under the supposition that ordered superconducting CuO_2 planes are necessary to allow the development of the superconductivity.

ACKNOWLEDGMENTS

The authors wish to thank P. G. Medaglia and A. A. Varlamov for useful discussions. This work was supported by PRA HTSS of INFM.

*Corresponding author. Permanent address: CONICET–Departamento de Fisica, Facultad de Ciencias Exactas, Universidad de Buenos Aires, Ciudad Universitaria, 1429 Buenos Aires, Argentina. Email: gpmm@bigfoot.com

[1] See, for instance, H. M. Christen, E. D. Specht, D. P. Norton, M. F. Chisholm, and L. A. Boatner, Appl. Phys. Lett. **72**, 2535 (1998).

[2] P. A. Salvador, A. M. Haghiri-Gosnet, B. Mercey, M. Hervieu, and B. Raveau, Appl. Phys. Lett. **75**, 2638 (1999).

[3] J. Fontcuberta, M. Bibes, B. Martinez, V. Trtik, C. Ferrater, F. Sanchez, and M. Varela, Appl. Phys. Lett. **74**, 1743 (1999).

[4] G. Balestrino, A. Crisan, S. Martellucci, P. G. Medaglia, A. Paoletti, and G. Petrocelli, in *Superconducting Superlattices II: Native and Artificial*, edited by I. Bozovic and D. Pavuna, Proc. SPIE Vol. 3480 (SPIE, Bellingham, WA, 1998), p. 37.

[5] M. Varela, Z. Sefrioui, D. Arias, M. A. Navacerrada, M. Lucia, M. A. Lopez de la Torre, C. Neon, G. D. Loos, F. Sanchez Quesada, and J. Santamaria, Phys. Rev. Lett. **83**, 3936 (1999).

[6] See, for instance, L. R. Tagirov, Phys. Rev. Lett. **83**, 2058 (1999); A. M. Grishin, S. I. Kartshew, and P. Johnsson, Appl. Phys. Lett. **74**, 1015 (1999); C. H. Ahn, S. Gariglio, P. Paruch, T. Tybell, L. Antognazza, and J. M. Triscone, Science **284**, 1152 (1999).

[7] See, for instance, Z. L. Wang, *Reflection Electron Microscopy and Spectroscopy for Surface Analysis* (Cambridge University Press, Cambridge, England, 1996).

[8] I. K. Schuller, M. Grimsditch, F. Chambers, G. Devane, H. Vanderstraeten, D. Neerinck, J. P. Locquet, and Y. Bruynseraede, Phys. Rev. Lett. **65**, 1235 (1990).

[9] E. E. Fullerton, I. K. Schuller, H. Vanderstraeten, and Y. Bruynseraede, Phys. Rev. B **45**, 9292 (1992).

[10] T. Fukui and H. Saito, Jpn. J. Appl. Phys., Part 2 **23**, L521 (1984).

[11] J. P. Locquet, D. Neerinck, L. Stokman, Y. Bruynseraede, and I. K. Schuller, Phys. Rev. B **38**, 3572 (1988).

[12] G. Balestrino, S. Martellucci, P. G. Medaglia, A. Paoletti, and G. Petrocelli, Physica C **302**, 78 (1998).

[13] G. Balestrino, A. Crisan, S. Lavanga, P. G. Medaglia, G. Petrocelli, and A. A. Varlamov, Phys. Rev. B **60**, 10504 (1999).
[14] S. Colonna, F. Arciprete, A. Balzarotti, G. Balestrino, P. G. Medaglia, and G. Petrocelli, Physica C (to be published).
[15] L. De Caro, C. Giannini, M. Nacucchi, L. Tapfer, G. Balestrino, P. G. Medaglia, and G. Petrocelli, Phys. Rev. B **59**, 14074 (1999).
[16] G. Balestrino, R. Desfeux, S. Martellucci, A. Paoletti, G. Petrocelli, A. Tebano, B. Mercey, and M. Hervieu, J. Mater. Chem. **5**, 1879 (1995).
[17] G. Balestrino, S. Martellucci, P. G. Medaglia, A. Paoletti, G. Petrocelli, and A. A. Varlamov, Phys. Rev. B **58**, R8925 (1998).
[18] C. Aruta, G. Balestrino, R. Desfeux, S. Martellucci, A. Paoletti, and G. Petrocelli, Appl. Phys. Lett. **68**, 926 (1996).